

Coefficient of Performance for Thermoelectric Thomson Device

Takahiro Chiba,¹ Ryo Iguchi,² Takashi Komine,³ Yasuhiro Hasegawa,⁴ and Ken-ichi Uchida^{2,5,6}

¹National Institute of Technology, Fukushima College, 30 Nagao,
Kamiarakawa, Taira, Iwaki, Fukushima 970-8034, Japan

²National Institute for Materials Science, Tsukuba, Ibaraki 305-0047, Japan

³Graduate School of Science and Engineering, Ibaraki University,
4-12-1 Nakanarusawa, Hitachi, Ibaraki 316-8511, Japan

⁴Graduate School of Science and Engineering, Saitama University,
255 Shimo-Okubo, Sakura-ku, Saitama 338-8570, Japan

⁵Institute for Materials Research, Tohoku University, Sendai, Miyagi 980-8577, Japan

⁶Center for Spintronics Research Network, Tohoku University, Sendai, Miyagi 980-8577, Japan

(Dated: March 16, 2022)

The Thomson effect induces heat release or absorption under the simultaneous application of a charge current and a temperature gradient to conductors. Although a thermoelectric Thomson device can be a simple temperature modulator without constructing heterojunction structure, in contrast to the Seebeck and Peltier effects, the thermoelectric performance of the Thomson effect driven by an external temperature difference has not been formulated so far. Here, we present an efficiency formula, i.e., coefficient of performance (COP) for the Thomson device. Based on the formulation, we find that COP of the Thomson device is characterized not only by the Thomson coefficient but also by the Seebeck coefficient. We show that the Thomson device can exhibit large COP for the cooling operation even if the conductor has a small Seebeck coefficient. We also present a more realistic discussion on COP of the Thomson device with material parameters. The proposed formula will provide a new guideline for finding thermoelectric materials.

I. INTRODUCTION

The linear-response thermoelectric phenomena, i.e., the Seebeck and Peltier effects, have been studied in the fundamental physics for more than a century and also used in a wide range of applications including energy harvesting and thermal management [1–5]. In terms of thermodynamics, a Seebeck power generator that converts heat into electrical work is interpreted as a thermoelectric engine (or the Carnot cycle) described by an efficiency whereas a Peltier temperature modulator corresponds to the inverse cycle with the coefficient of performance (COP). The formula for maximum efficiency (η^{\max}) and maximum COP of such thermoelectric devices are characterized by the dimensionless figure of merit [1]

$$ZT = \frac{S^2}{\rho\kappa}T, \quad (1)$$

which is used to design better thermoelectric materials for practical device applications. Here, ZT is defined based on the assumption of temperature (T) independent transport coefficients: the Seebeck coefficient (S), electrical resistivity (ρ), and thermal conductivity (κ). Because of this assumption, the calculated η^{\max} based on ZT often leads to over- or under-estimation. To avoid the issue, recently, the concept of ZT has been generalized to the case with a large temperature difference (ΔT) between the hot and cold sides by introducing an engineering figure of merit [6]

$$(ZT)_{eng} = \frac{\langle S \rangle_T^2}{\langle \rho \rangle_T \langle \kappa \rangle_T} \Delta T, \quad (2)$$

where $\langle C \rangle_T = (1/\Delta T) \int_{T_c}^{T_h} C(T) dT$ ($C = S, \rho, \kappa$) and $\Delta T = T_h - T_c$ with T_h and T_c being the hot- and cold-side temperatures, respectively. Owing to this treatment, without the complex numerical simulation that gives an accurate efficiency,

one can predict a more realistic efficiency in practical operating conditions under the large temperature difference. However, practical applications of the linear-response thermoelectric phenomena involve structuring and/or durability issues. For example, since the Peltier device has a complicated cascade structure consisting of two dissimilar thermoelectric materials, it has not reached a wide range of applications.

Unlike the Peltier device with the complicated cascade structure, a thermoelectric device based on the Thomson effect (Thomson device) works as a simple temperature modulator without constructing heterojunction structure. The Thomson effect, one of the nonlinear thermoelectric phenomena, induces heat release or absorption under the simultaneous application of a charge current density \mathbf{J} and a temperature gradient ∇T to conductors. The induced heat production rate per unit volume is given by

$$q = -\tau(T)\mathbf{J} \cdot \nabla T, \quad (3)$$

where

$$\tau(T) = T \frac{dS}{dT} \quad (4)$$

is the Thomson coefficient. Equation (4) indicates that conductors with a sharp T dependence of S are potential candidates to generate the large Thomson effect. Recently, Modak *et al.* found that due to the steep T dependence of the Seebeck coefficient, FeRh-based alloys show huge values of the Thomson coefficient approaching $\sim 1000 \mu\text{VK}^{-1}$ around room temperature [7]. They demonstrated that the Thomson-effect-induced cooling can be larger than the Joule heating in the FeRh-based alloy in a steady state. Furthermore, Uchida *et al.* reported that the magnitude of the Thomson-effect-induced temperature change in $\text{Bi}_{88}\text{Sb}_{12}$ is strongly enhanced by applying a magnetic field [8]. Hence, control of the local temperature and COP by the Thomson effect might be a potential

technology for nonlinear thermoelectrics and spin caloritronics. Although the influence of the Thomson effect driven by an internal temperature gradient in a Peltier device has been theoretically discussed [9–11], the performance of the thermoelectric device operated by the Thomson effect under an external temperature difference has not been formulated so far. Thus, the thermal management based on the Thomson effect needs to develop not only materials science but also fundamental physics.

In this paper, we propose an efficiency formula, i.e., COP for a thermoelectric Thomson device. We discuss the Thomson device in terms of thermodynamics and reveal important factors that characterize the device operation, followed by estimating COP of the Thomson device with realistic thermoelectric coefficients of several materials. We show that the Thomson device can exhibit large COP for the cooling operation even if the conductor has a small Seebeck coefficient.

The outline of the paper is as follows. In Sec. II, we construct a formulation of COP for the Thomson device by starting from COP of an electric heater and subsequently taking into account the linear- and nonlinear-response thermoelectric effects. In Sec. III, we analyze the formulated COP and a local temperature by solving a heat equation. We also present a more realistic discussion on COP of the Thomson device with material parameters. Finally, in Sec. IV, we summarize and conclude this work.

II. FORMULATION

In this section, we construct a formulation of COP for the Thomson device. We start from the calculation for an electric heater characterized by COP for the thermally isolated system. We subsequently take into account the Seebeck and Thomson effects in the COP and present a COP formula for the Thomson device that is a thermally closed system, i.e., the system that has an external temperature difference via interacting to a heat bath.

A. Model

We consider a single thermoelectric element (with the cross-sectional area A and the length L) connected with a perfect conductor wiring at both the ends, as shown in Fig. 1. Without loss of generality, we restrict thermoelectric transports to one spatial dimension. In the presence of an electric field (E_x) and a temperature gradient ($-dT/dx$) along the x -axis, charge and heat current densities are respectively described as,

$$J = \sigma(T)E_x - \sigma(T)S(T)\frac{dT}{dx}, \quad (5)$$

$$J_Q = S(T)TJ - \kappa(T)\frac{dT}{dx}, \quad (6)$$

where $\sigma(T) = \rho^{-1}(T)$ is the electrical conductivity.

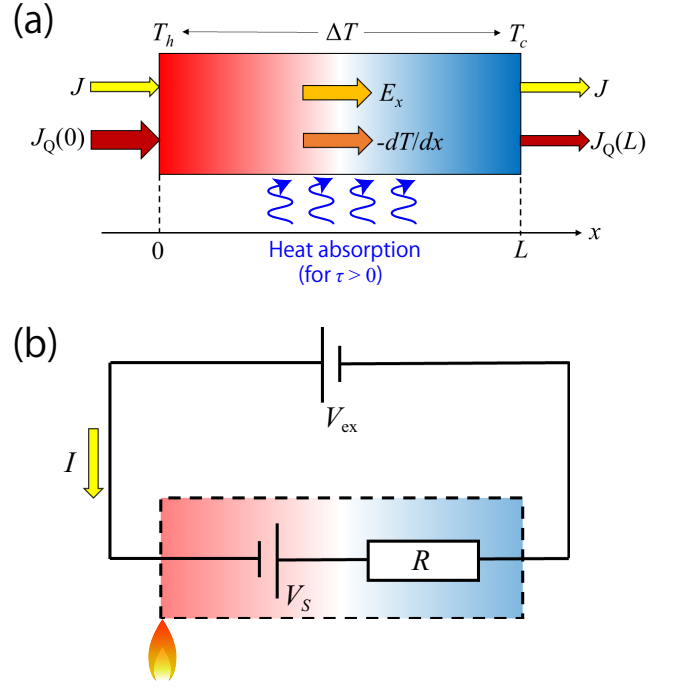


FIG. 1. (a) Schematic of a single thermoelectric element (Thomson device) in the one-dimensional geometry in which T_h and T_c denote the hot- and cold-side temperatures, respectively. (b) The equivalent circuit model of the Thomson device. V_{ex} is an external voltage and V_S a voltage generated by the Seebeck effect. The other parameters are defined in the text.

Applying thermodynamics to thermoelectric phenomena, the first law of thermodynamics for Fermi gas gives the expression of the total energy current density [3]

$$J_U = J_Q + \frac{\mu_e}{e}J, \quad (7)$$

where e is the elemental charge and μ_e the electrochemical potential. These current densities are conjugated to their thermodynamic potential gradients or general forces driven from the thermodynamic potentials. Then, the energy balance over the thermoelectric element is governed by

$$\frac{dJ_Q}{dx} = E_x J, \quad (8)$$

where we use the energy and particle conservations

$$\frac{dJ_U}{dx} = 0, \quad (9)$$

$$\frac{dJ}{dx} = 0, \quad (10)$$

and $E_x = -(1/e)d\mu_e/dx$. By using Eqs. (5) and (6), the electrical power production and the energy balance can be expressed as

$$E_x J = \rho(T)J^2 + S(T)\frac{dT}{dx}J, \quad (11)$$

$$\frac{dJ_Q}{dx} = \rho(T)J^2 - \tau(T)\frac{dT}{dx}J, \quad (12)$$

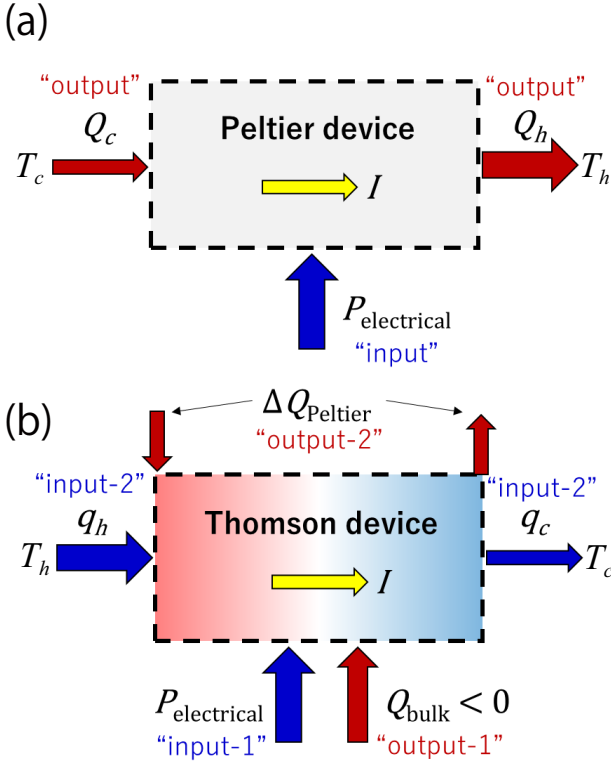


FIG. 2. (a) Energy diagram of the Peltier device as a temperature modulator utilizing “interfacial heat” which corresponds to $\Delta Q_{\text{Peltier}}$ in (b). Applied power $P_{\text{electrical}}$ satisfies $P_{\text{electrical}} = -(Q_h - Q_c)$. (b) Energy diagram of the Thomson device as a temperature modulator utilizing “bulk heat”. Sum of applied powers $P_{\text{electrical}} + q_h - q_c$ satisfies $P_{\text{electrical}} + q_h - q_c = \Delta Q_{\text{Peltier}} + Q_{\text{bulk}}$, where $\Delta Q_{\text{Peltier}}$ indicates a balance of Peltier heats in the device. Current-induced cooling ($Q_{\text{bulk}} < 0$) occurs when a heat absorption by the Thomson effect is larger than the Joule heating. The detail of these operations are described in the text.

where $J_{\kappa} = -\kappa(T)(dT/dx)$ is a Fourier heat current density. In contrast to the Joule heating that is proportional to J^2 , the Thomson term is proportional to J , enabling the control of heat release or absorption depending on whether a charge current flows in the direction parallel or antiparallel to a temperature gradient. Importantly, the sign and magnitude of the Thomson term are determined by $\tau(T)$.

B. COP

Based on the energy balance governed by Eq. (8), heaters and coolers are characterized by COP

$$\phi = \frac{Q}{P}, \quad (13)$$

where

$$P = A \int_0^L \frac{dJ_Q}{dx} dx \quad (14)$$

is the power applied to the device and Q is the output heat power.

As shown in Fig. 2 (a), the Peltier device is equivalent to the inverse Carnot cycle (or heat pump) of the Fermi gas [3, 9]. Hence, the output heat powers are described by

$$Q_h \equiv Q = -AJ_Q(L) \quad (\text{for heater}), \quad (15)$$

$$Q_c \equiv Q = -AJ_Q(0) \quad (\text{for cooler}), \quad (16)$$

respectively, and then the applied electrical power satisfies (see Appendix A)

$$P_{\text{electrical}} = -(Q_h - Q_c). \quad (17)$$

In this sense, the Peltier device is a temperature modulator utilizing “interfacial heat” which consists of the Peltier heat at the junction and a heat diffusion into the bulk (see Eqs. (A6) and (A7)). Then, each COP is defined by

$$\phi_P^{(h)} = \frac{Q_h}{P_{\text{electrical}}} \quad (\text{for heater}), \quad (18)$$

$$\phi_P^{(c)} = \frac{Q_c}{P_{\text{electrical}}} \quad (\text{for cooler}). \quad (19)$$

In contrast, traditional electric heaters are temperature modulators utilizing “bulk heat”. For example, an electric heater converts electricity into heat via Joule’s first law in the bulk. Similarly, the Thomson device electrically controls heat release or absorption by using the Thomson effect. Hence, for such temperature modulators, we define the output heat power

$$Q_{\text{bulk}} \equiv Q = A \int_0^L \frac{dJ_{\kappa}}{dx} dx. \quad (20)$$

Since both the temperature gradient and charge current are the driving forces for the Thomson effect, electrical work interacting with the external temperature difference should be taken into account in the the applied power. Based on this insight, as described in Fig. 2 (b), we add the corresponding energy consumption ($q_h - q_c$) to the energy diagram of the Peltier device, which corresponds to taking into account an operation of the Seebeck power generator. Then, sum of applied powers to the Thomson device is defined by

$$P_T \equiv P_{\text{electrical}} + q_h - q_c. \quad (21)$$

This treatment reflects the fact that the Thomson effect originates from the simultaneous operation of the Peltier and Seebeck effects in the device. By using Eq. (17), P_T can be rewritten as

$$\begin{aligned} P_T &= q_h - Q_h - (q_c - Q_c) \\ &= \tilde{q}_h - \tilde{q}_c, \end{aligned} \quad (22)$$

where we define $\tilde{q}_{h(c)} \equiv q_{h(c)} - Q_{h(c)}$, which satisfies the general relation of an applied power (see Eq. (14)). On the other hand, according to Eq. (6), we can also divide the applied power into interfacial and bulk heat contributions

$$\begin{aligned} P_T &= A \int_0^L \frac{d}{dx} \left(S(T)TJ - \kappa(T) \frac{dT}{dx} \right) dx \\ &= -I [\Pi(T)]_0^L + Q_{\text{bulk}}, \end{aligned} \quad (23)$$

where $I = AJ$ is a charge current and $\Pi(T) = TS(T)$ is the Pelter coefficient. For the Thomson device, as shown in Fig. 2 (b), the applied power satisfies $P_T = \Delta Q_{\text{Peltier}} + Q_{\text{bulk}}$, where $\Delta Q_{\text{Peltier}} = -I[\Pi(T)]_0^L$ indicates a balance of Peltier heats in the device. Therefore, we define COP of the Thomson device by

$$\phi_T = \frac{Q_{\text{bulk}}}{P_T}. \quad (24)$$

Hereafter, we construct a formulation of COP for the Thomson device based on Eq. (24).

1. Electric heater

Once apart from the thermoelectric property in materials, it is constructive to consider COP of traditional electric heaters which can be approximately regarded as the thermally isolated system, i.e., the system without an external temperature difference. These devices convert electricity into heat via Joule's first law in the bulk. Hence, we assume a weak T dependence of $\rho(T)$ and $S = 0$ in Eq. (12) so that the applied and output heat powers are respectively given by

$$\begin{aligned} P_J &= A \int_0^L \frac{dJ_Q}{dx} dx \\ &= A \int_0^L E_x J dx \\ &= A \int_0^L \rho J^2 dx = RI^2, \end{aligned} \quad (25)$$

$$\begin{aligned} Q_J &= Q_{\text{bulk}} \\ &= A \int_0^L \rho J^2 dx = RI^2, \end{aligned} \quad (26)$$

where $R = \langle \rho \rangle_T L/A \approx \rho L/A$ is the electrical resistance and $I = AJ$ is a charge current. Accordingly, COP of the electric heater is always unity as

$$\phi_J = \frac{Q_J}{P_J} = 1. \quad (27)$$

2. Electric heater including the Seebeck effect

Next, we integrate the Seebeck effect into the traditional electric heater. Hereafter, we consider a thermally closed system, i.e., the system that has an external temperature difference via interacting to a heat bath. Assuming a weak T dependence of the electrical resistivity and Seebeck coefficient, i.e., $\tau(T) \approx 0$, in Eq. (12), the applied and output heat powers

are respectively given by

$$\begin{aligned} P_S &= A \int_0^L \frac{dJ_Q}{dx} dx \\ &= A \int_0^L E_x J dx \\ &= A \int_0^L \left(\rho J^2 + S \frac{dT}{dx} J \right) dx \\ &= RI^2 - S \Delta T I, \end{aligned} \quad (28)$$

$$\begin{aligned} Q_S &= Q_{\text{bulk}} \\ &= A \int_0^L \rho J^2 dx = RI^2, \end{aligned} \quad (29)$$

where we use $E_x = \rho J + S (dT/dx)$ and $\int_0^L (dT/dx) dx = \int_{T_h}^{T_c} dT = -\Delta T$. Then, COP is calculated by

$$\phi_S = \frac{Q_S}{P_S} = 1 + \frac{S \Delta T I}{RI^2 - S \Delta T I}. \quad (30)$$

Equation (30) indicates that COP of the electric heater deviates from unity depending on the sign of S and the relative relation (parallel or antiparallel) between the J and $-dT/dx$ directions.

3. Electric heater including the Thomson effect: Thomson device

Here, according to Eq. (12), we take into account the Thomson effect in the electric heater, leading to the applied and output heat powers respectively being

$$\begin{aligned} P_T &= A \int_0^L \frac{dJ_Q}{dx} dx \\ &= A \int_0^L E_x J dx \\ &= A \int_0^L \left(\rho(T) J^2 + S(T) \frac{dT}{dx} J \right) dx \\ &= \langle \rho \rangle_x \frac{L}{A} I^2 - \langle S \rangle_T \Delta T I, \end{aligned} \quad (31)$$

$$\begin{aligned} Q_T &= Q_{\text{bulk}} \\ &= A \int_0^L \left(\rho(T) J^2 - \tau(T) \frac{dT}{dx} J \right) dx \\ &= \langle \rho \rangle_x \frac{L}{A} I^2 + \langle \tau \rangle_T \Delta T I, \end{aligned} \quad (32)$$

where

$$\langle \rho \rangle_x = \frac{1}{L} \int_0^L \rho(T) dx. \quad (33)$$

We also use $E_x = \rho(T)J + S(T)(dT/dx)$ and Eq. (4). Note that

$$\begin{aligned} \langle \tau \rangle_T &= \frac{1}{\Delta T} \int_{T_c}^{T_h} T \frac{dS}{dT} dT \\ &= \frac{1}{\Delta T} [TS(T)]_{T_c}^{T_h} - \frac{1}{\Delta T} \int_{T_c}^{T_h} S(T) dT \\ &= \frac{\Pi(T_h) - \Pi(T_c)}{\Delta T} - \langle S \rangle_T, \end{aligned} \quad (34)$$

which reflects the first Thomson (or Kelvin) relation. The relation Eq. (34) leads to $P_T = -(\Pi(T_h) - \Pi(T_c))I + Q_T$, which means that the applied power P_T is distributed into an interfacial heat $-(\Pi(T_h) - \Pi(T_c))I$ and a bulk heat Q_T . Then, COP is calculated by

$$\phi_T = \frac{Q_T}{P_T} = 1 + \frac{(\langle \tau \rangle_T + \langle S \rangle_T) \Delta T I}{W_J R I^2 - \langle S \rangle_T \Delta T I}, \quad (35)$$

where

$$W_J = \frac{\frac{1}{L} \int_0^L \rho(T) dx}{\frac{1}{\Delta T} \int_{T_c}^{T_h} \rho(T) dT}. \quad (36)$$

When the Thomson term in Eq. (12) is negative, Eq. (35) indicates that the Thomson term increases ϕ_T compared to Eq. (30). In contrast, when the Thomson term in Eq. (12) is positive and greater than the Joule heating term, the Thomson effect generates heat absorption ($Q_T < 0$) in the bulk. For example, such a situation can be realized when for $\langle \tau \rangle_T > 0$ a charge current flows in the antiparallel direction of a temperature gradient. Then, the Thomson device works as a cooler, which is characterized by $\phi_T < 0$. We would like to mention the electrical power for generating the external temperature difference. In the current formulation, we assume the existence of the external temperature difference, i.e. a Thomson device connected to two heat baths with different temperatures. If the temperature difference is necessary generated by applying a power, e.g. using a heater, such energy consumption should be taken into consideration.

III. DISCUSSION

In the previous section, we have formulated COP with the heating or cooling contribution induced by the Thomson effect. This treatment is essentially different from the previously reported model that incorporates the contribution of the Thomson term into the Peltier device [9, 10]. In this section, we show how the formulated COP and a local temperature $T(x)$ of the Thomson device depend on the transport coefficients.

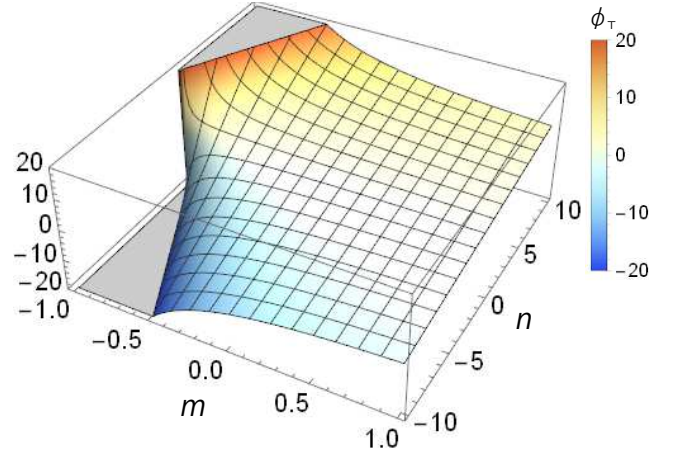


FIG. 3. COP of thermoelectric Thomson cooler as a function of $m (= \langle S \rangle_T \Delta T / (RI))$ and $n (= \langle \tau \rangle_T \Delta T / (RI))$.

A. Analysis of COP

We analyze ϕ_T by using the following dimensionless parameters

$$m = \frac{\langle S \rangle_T \Delta T}{RI}, \quad (37)$$

$$n = \frac{\langle \tau \rangle_T \Delta T}{RI}. \quad (38)$$

Then, Eq. (35) is rewritten as

$$\phi_T = 1 + \frac{n + m}{W_J + m}. \quad (39)$$

We investigate how COP of the Thomson device depends on the dimensionless parameters (m, n). For simplicity, we set $W_J = 1$ by assuming a weak T dependence of the electrical resistivity ($d\rho/dT \approx 0$). Figure 3 shows the calculated COP in the case of both heating ($\phi_T > 0$) and cooling ($\phi_T < 0$). As seen, COP is enhanced by larger $|n|$ and $m \rightarrow -1$ ($-W_J$). Hence, for high-performance heating operation of the Thomson device, one will seek a material having large $\langle \tau \rangle_T$ and $\langle S \rangle_T$ with the same sign. In contrast, for high-performance cooling operation, one may need a material having a much larger $\langle \tau \rangle_T$ than $\langle S \rangle_T$ with the opposite sign to each other.

B. Local temperature $T(x)$ of the Thomson device

Here, we investigate how the local temperature $T(x)$ of the Thomson device depends on the transport coefficients by solving Eq. (12). Assuming a weak T dependence of the thermal conductivity ($d\kappa/dT \approx 0$) and $\Delta T \ll T$, we replace Eq. (12) by the following heat equation with temperature averaged thermoelectric coefficients:

$$\frac{d^2 T}{dx^2} = -\frac{\langle \rho \rangle_T}{\langle \kappa \rangle_T} J^2 + \frac{\langle \tau \rangle_T}{\langle \kappa \rangle_T} \frac{dT}{dx} J, \quad (40)$$

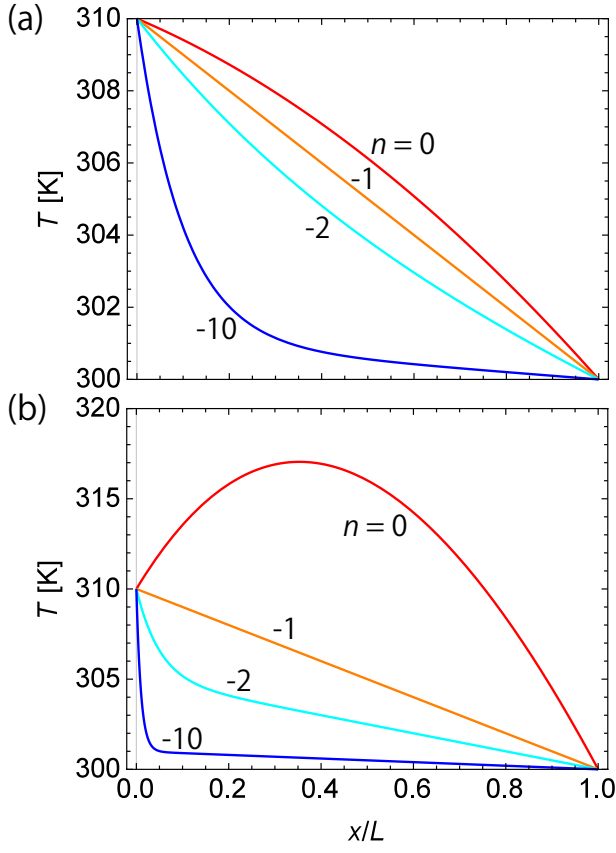


FIG. 4. Local temperature as a function of a normalized position x/L for different values of n ($= \langle \tau \rangle_T \Delta T / (RI)$) with (a) $c_\kappa = 1$ and (b) $c_\kappa = 0.1$. In these plots, $T_c = 300$ K and $\Delta T = 10$ K are used.

which gives

$$T(x) = T_h + \frac{\Delta T}{n} \frac{x}{L} - \Delta T \left(1 + \frac{1}{n} \right) \frac{e^{\frac{n}{c_\kappa} \frac{x}{L}} - 1}{e^{\frac{n}{c_\kappa}} - 1} \quad (41)$$

with

$$c_\kappa = \frac{K \Delta T}{RI^2}, \quad (42)$$

where $K = \langle \kappa \rangle_T A / L$ is the thermal conductance. Here, we set the thermal boundary condition as $T(x=0) = T_h = \Delta T + T_c$ and $T(x=L) = T_c$ in Fig. 1 (a). Note that the influence of thermal boundary conditions are discussed in Appendix B.

As a typical situation, we consider the cooling operation of the Thomson device. The simplest case can be realized when for $\langle \tau \rangle_T > 0$ a charge current flows in the antiparallel direction of a temperature gradient. To describe such a situation, we set the opposite current direction to the temperature gradient, i.e. $-I$, but keep the thermal boundary condition in Fig. 1 (a). Figure 4 shows a numerical solution of the local temperature $T(x)$ for different values of n and c_κ . In the case of $c_\kappa \sim 1$ and $n \sim -1$, the temperature gradient is almost uniform along the x -axis and can be approximated by

$$\frac{dT}{dx} \approx -\frac{\Delta T}{L}, \quad (43)$$

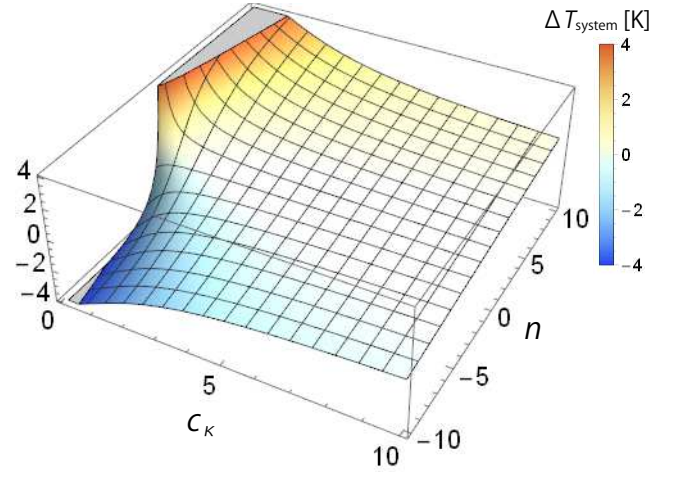


FIG. 5. System temperature difference as a function of c_κ ($= K \Delta T / (RI^2)$) and n ($= \langle \tau \rangle_T \Delta T / (RI)$). In this plots, $T_c = 300$ K and $\Delta T = 10$ K are used.

which means that the temperature gradient is dominantly due to a Fourier heat (J_κ). In the case of a relatively small $c_\kappa = 0.1$, the temperature gradient has nonlinear x -dependence. For $n \sim 0$, the Joule heating is dominant, making $T(x)$ be a well-known convex parabola distribution. On the other hand, for $n \ll -1$, the Thomson cooling overcomes the Joule heating so that $T(x)$ can be approximated by

$$T(x) \approx T_h - \Delta T \frac{\exp\left(\frac{\langle \tau \rangle_T J x}{\langle \kappa \rangle_T}\right) - 1}{\exp\left(\frac{\langle \tau \rangle_T J L}{\langle \kappa \rangle_T}\right) - 1}. \quad (44)$$

Note that $T(x) \geq T_c$ within $0 \leq x/L \leq 1$ for $n \rightarrow -\infty$.

C. System temperature difference ΔT_{system}

To characterize the Thomson device as a temperature modulator, we introduce a system temperature difference ΔT_{system} measured from $(T_h + T_c) / 2$, which is defined by

$$\Delta T_{\text{system}} = \langle T \rangle_x - \frac{T_h + T_c}{2}, \quad (45)$$

where

$$\langle T \rangle_x = \frac{1}{L} \int_0^L T(x) dx \quad (46)$$

is an averaged temperature across the device and $(T_h + T_c) / 2$ corresponds to $\langle T \rangle_x$ for the uniform temperature gradient (see Eq. (43)). Hence, $\Delta T_{\text{system}} < 0$ means that the system is cooled down by the Thomson effect. Calculated ΔT_{system} in the case of both heating and cooling is shown in Fig. 5. For cooling (heating) the system temperature, negatively (positively) larger n and smaller c_κ are desirable, which reflects the n dependence behavior of COP in Fig. 3. Hence, for high-performance operation of the Thomson device, one will seek a material having larger $|\langle \tau \rangle_T|$ and smaller $\langle \kappa \rangle_T$. Taking into

TABLE I. Parameters for Pt.

	Symbol	Value	Unit
^a Electrical resistivity	$\langle\rho\rangle_T$	1.1×10^{-7}	Ωm
^a Seebeck coefficient	$\langle S\rangle_T$	-4.8	μVK^{-1}
^a Thomson coefficient	$\langle\tau\rangle_T$	-8.6	μVK^{-1}
^a Thermal conductivity	$\langle\kappa\rangle_T$	71.6	$\text{Wm}^{-1}\text{K}^{-1}$
^b Dimensionless parameter	m	-0.8×10^{-3}	
^b Dimensionless parameter	n	-1.4×10^{-3}	
^b Dimensionless parameter	c_κ	1.1	
COP	ϕ_T	1.00	
System temperature difference	ΔT_{system}	0.39	K

^aReference 12, ^bFor $\Delta T = 10$ K, $L = 14$ mm, $I \approx 0.3$ A.

account this point, we perform further investigations in the next section by using realistic thermoelectric coefficients for various materials.

D. Material requirements

In this section, we estimate the local temperature and COP of the Thomson device by using realistic thermoelectric coefficients for Pt, Bi_2Te_3 , and FeRh-based alloy [7]. We also investigate an influence on the local temperature and COP from the magneto-Thomson effect in BiSb alloy [8].

1. Pt

Pt is most widely used as a reference to determine the Seebeck coefficient of thermoelectric materials [12]. Calculated COP and system temperature difference are listed in Table I. As seen, the system temperature slightly increases by $\Delta T_{\text{system}} = 0.25$ K, which is due to a small electrical resistivity, not to the Thomson effect induced cooling. This result is reflected by $\phi_T = 1.00$.

2. Bi_2Te_3

Bismuth telluride, Bi_2Te_3 , is a commercial material typically used for the Peltier cooler and Seebeck power generator because Bi_2Te_3 has the top-level value of ZT around room temperature [13]. Furthermore, a relatively large Thomson coefficient $\sim 150 \mu\text{VK}^{-1}$ at 300 K is predicted in a p-type Bi_2Te_3 by experiments [13] and first-principles calculation [14]. This Thomson coefficient could be even more enhanced for wide-gap semiconductors with very low carrier concentrations [10, 14]. However, as seen in Table II, the low carrier concentrations lead to increasing of electrical resistivity, which generates a huge Joule heating reflected by $\phi_T = 0.92$. Consequently, even with a relatively large $(ZT)_{\text{eng}} = 0.02$ and the Thomson coefficient, the heat absorption by the Thomson effect becomes negligible and Bi_2Te_3 is ineligible for cooling applications based on the Thomson device.

TABLE II. Parameters for Bi_2Te_3 .

p -type ($T = 300$ K)	Symbol	Value	Unit
^a Electrical resistivity	$\langle\rho\rangle_T$	7.5×10^{-6}	Ωm
^{ab} Seebeck coefficient	$\langle S\rangle_T$	170	μVK^{-1}
^{ab} Thomson coefficient	$\langle\tau\rangle_T$	150	μVK^{-1}
^c Thermal conductivity	$\langle\kappa\rangle_T$	1.9	$\text{Wm}^{-1}\text{K}^{-1}$
^d Dimensionless parameter	m	-0.040	
^d Dimensionless parameter	n	-0.036	
^d Dimensionless parameter	c_κ	0.060	
COP	ϕ_T	0.92	
System temperature difference	ΔT_{system}	10	K

^aReference 13, ^bReference 14, ^cReference 15, ^dFor $\Delta T = 10$ K, $L = 14$ mm, $I \approx -0.3$ A.

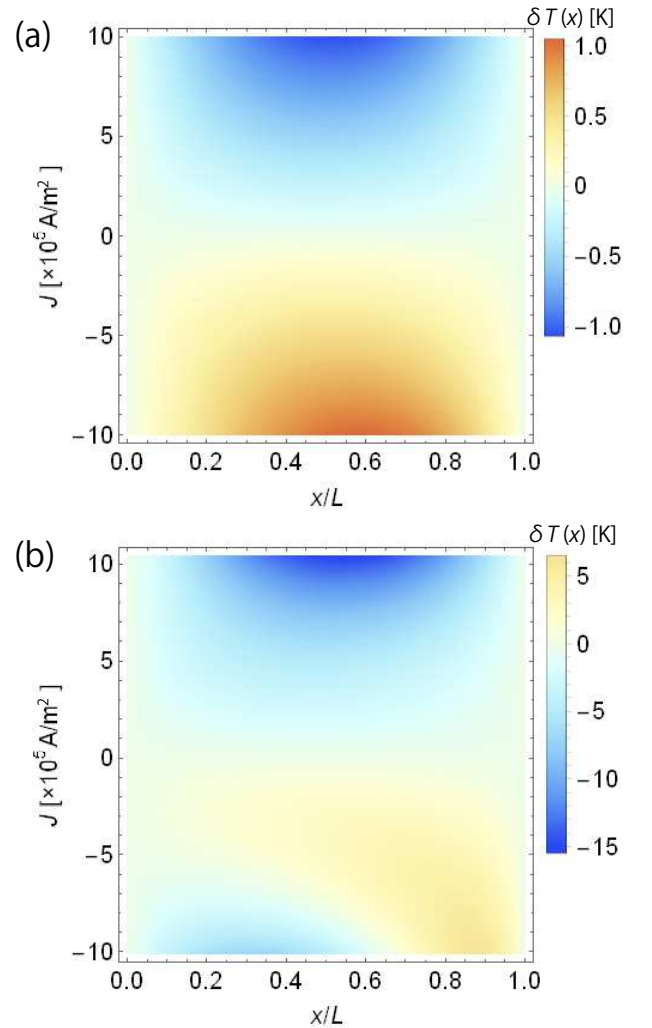


FIG. 6. Local temperature difference $\delta T(x)$ in a FeRh-based alloy as a function of a normalized position x/L and a charge current density J for (a) $\langle\kappa\rangle_T = 15 \text{ Wm}^{-1}\text{K}^{-1}$ and (b) $\langle\kappa\rangle_T = 1.5 \text{ Wm}^{-1}\text{K}^{-1}$ (assumption). In these plots, $T_c = 312$ K and $\Delta T = 10$ K are used. The other parameters are listed in Tables III. The definition of $\delta T(x)$ (see Eq. (47)) is explained in the text.

3. FeRh-based alloy

FeRh-based alloys are well-studied magnetic materials that exhibit a first-order antiferromagnetic-ferromagnetic phase transition around room temperature [16]. This phase transition accompanies a steep T dependence of the transport properties [17, 18]. Recently, due to the steep T dependence of the Seebeck coefficient, it is found that FeRh-based alloys show huge values of the Thomson coefficient approaching $\sim 1000 \mu\text{VK}^{-1}$ around room temperature [7]. To elucidate how the Thomson effect modifies the local temperature, we define a local temperature difference in the presence/absence of the Thomson effect

$$\delta T(x) = T(x) - T(x)|_{\tau=0}, \quad (47)$$

where $T(x)|_{\tau=0}$ denotes the local temperature in the absence of the Thomson effect. Figure 6 shows calculated $\delta T(x)$ for a FeRh-based alloy with material parameters listed in Table III. Note that in actual the phase-transition-induced giant Thomson coefficient in Table III is obtained within a narrow temperature range (a several Kelvin) but for simplicity we assume keeping the highest value in our calculation. As seen in Fig. 6 (a), the Thomson-effect-induced cooling (for $J > 0$) and heating (for $J < 0$) become maxim around the center ($x/L = 0.5$) of the device. For $J > 0$, although the FeRh-based alloy has a relatively high electrical resistivity compared with pure metals, the Joule heating is suppressed by the Thomson-effect-induced cooling, which is characterized by $\phi_T = -0.57$. Consequently, the system is cooled down and obtains $\Delta T_{\text{system}} = -0.10$ K. As shown in this example, the Thomson-effect-induced cooling is possible even when the Seebeck coefficient and $(ZT)_{\text{eng}}$ ($\sim 10^{-4}$ for FeRh-based alloys) are small, which is also confirmed by a recent experiment [7]. If we can reduce the thermal conductivity down to $1.5 \text{ Wm}^{-1}\text{K}^{-1}$ without changing other parameters, the system is farther cooled down and obtains $\Delta T_{\text{system}} = -0.83$ K. Corresponding temperature modulation by the Thomson effect is shown in Fig. 6 (b). As seen, current reversal shows an asymmetry in the Thomson-effect-induced temperature modulation and the cooling operation is strongly enhanced. Even in the heating operation, the Thomson effect partially suppresses the Joule heating. These results indicate that the Thomson effect is more efficient in the cooling operation rather than the heating operation.

4. BiSb alloy

BiSb alloys ($\text{Bi}_{1-x}\text{Sb}_x$) show various solid-state phases such as semimetal, narrow-gap semiconductor, and three-dimensional topological insulator by tuning the composition x [19]. The thermomagnetic properties of BiSb alloys have also been studied intensively so far [20, 21]. In 2020, Uchida *et al.* reported that the Thomson coefficient of $\text{Bi}_{88}\text{Sb}_{12}$ is strongly enhanced by applying a magnetic field, as shown in Table IV. Here, we investigate an influence on the local temperature and COP from the magneto-Thomson effect in

TABLE III. Parameters for FeRh-based alloy.

	Symbol	Value	Unit
^a Electrical resistivity	$\langle \rho \rangle_T$	1.1×10^{-6}	Ωm
^a Seebeck coefficient	$\langle S \rangle_T$	-11	μVK^{-1}
^a Thomson coefficient	$\langle \tau \rangle_T$	-906	μVK^{-1}
^a Thermal conductivity	$\langle \kappa \rangle_T$	15	$\text{Wm}^{-1}\text{K}^{-1}$
^b Dimensionless parameter	m	-0.019	
^b Dimensionless parameter	n	-1.53	
^b Dimensionless parameter	c_κ	23	
COP	ϕ_T	-0.57	
System temperature difference	ΔT_{system}	-0.10	K

^aReference 7, ^bFor $\Delta T = 10$ K, $L = 14$ mm, $I \approx 0.3$ A.

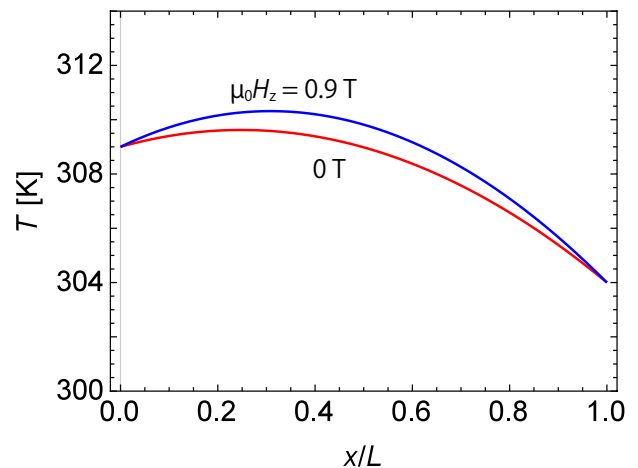


FIG. 7. Local temperature as a function of a normalized position x/L in a BiSb alloy in the presence/absence of a magnetic field $\mu_0 H_z$. In this plot, $T_c = 304$ K and $\Delta T = 5$ K are used. The other parameters are listed in IV.

a BiSb alloy. Figure 7 shows calculated local temperature for $\text{Bi}_{88}\text{Sb}_{12}$ with material parameters listed in Table IV. In the presence of a magnetic field, the electrical resistivity increases due to the magnetoresistance effect, leading to an enhancement of Joule heating. Note that Thomson cooling is also enhanced by the magneto-Thomson effect but is less than that of the Joule heating. Consequently, the system temperature becomes higher than that of zero magnetic field case and obtains $\Delta T_{\text{system}} = 2.3$ K. Next, ϕ_T in the presence/absence of the magnetic field is shown in Table IV. In the presence of a magnetic field, the COP decreases due to the magnetic-field-induced enhancement of the Thomson coefficient. We find COP changing rate $1 - \phi_T(0.9 \text{ T})/\phi_T(0 \text{ T}) = 1.2 \%$. Therefore, for an efficient cooling owing to the magneto-Thomson effect, materials with a larger magnetic field dependence of the Thomson coefficient will be required. In this sense, three-dimensional topological insulator phase of BiSb alloys [19] and Bi_2Te_3 tetradymite family [13] might be potential candidates for the magneto-Thomson effect because of a drastic transport property change on a topological phase transition induced by a magnetic field [22, 23].

TABLE IV. Parameters for Bi₈₈Sb₁₂.

$\mu_0 H_z = 0$ T	Symbol	Value	Unit
^a Electrical resistivity	$\langle \rho \rangle_T$	3.1×10^{-6}	Ωm
^a Seebeck coefficient	$\langle S \rangle_T$	-91	μVK^{-1}
^a Thomson coefficient	$\langle \tau \rangle_T$	45	μVK^{-1}
^a Thermal conductivity	$\langle \kappa \rangle_T$	3.5	$\text{Wm}^{-1}\text{K}^{-1}$
^b Dimensionless parameter	m	0.031	
^b Dimensionless parameter	n	-0.015	
^b Dimensionless parameter	c_κ	0.34	
COP	ϕ_T	1.015	
System temperature difference	ΔT_{system}	1.7	K
<hr/>			
$\mu_0 H_z = 0.9$ T	Symbol	Value	Unit
^a Electrical resistivity	$\langle \rho \rangle_T$	3.8×10^{-6}	Ωm
^a Seebeck coefficient	$\langle S \rangle_T$	-110	μVK^{-1}
^a Thomson coefficient	$\langle \tau \rangle_T$	98	μVK^{-1}
^a Thermal conductivity	$\langle \kappa \rangle_T$	3.2	$\text{Wm}^{-1}\text{K}^{-1}$
^b Dimensionless parameter	m	0.030	
^b Dimensionless parameter	n	-0.027	
^b Dimensionless parameter	c_κ	0.20	
COP	ϕ_T	1.003	
System temperature difference	ΔT_{system}	2.3	K

^aReference 8, ^bFor $\Delta T = 10$ K, $L = 0.5$ mm, $I \approx -0.1$ A.

IV. SUMMARY

In summary, we have presented an efficiency formula, i.e., COP for a thermoelectric Thomson device by taking into account the nonlinearity of the thermoelectric effect due to the T dependence of the Seebeck coefficient. Based on the formulation, we have discussed the Thomson device in terms of thermodynamic system by revealing an important factor that characterizes the device operation. We also demonstrate that even if the material has a small Seebeck coefficient, which is not conventionally regarded as a thermoelectric material, the Thomson device can exhibit large COP for the cooling operation. Furthermore, we estimate the local temperature and COP of the Thomson device with realistic thermoelectric coefficients of several materials. It is demonstrated that the system can be cooled down by using parameters of a FeRh-based alloy. We have also investigated an influence on the local temperature and COP from the magneto-Thomson effect in a BiSb alloy. This work will be the basis for designing Thomson devices and for finding materials for nonlinear thermoelectrics and spin caloritronics.

V. ACKNOWLEDGMENTS

The authors thank Rajkumar Modak, Kei Yamamoto, and Gerrit. E. W. Bauer for valuable discussions. This work was supported by Grants-in-Aid for Scientific Research (Grant Nos. 20K15163, 20H02196, 21K18590, and 19H02585) from JSPS KAKENHI, Japan, and CREST "Creation of Innovative Core Technologies for Nano-enabled Thermal Man-

agement" (Grant No. JPMJCR1711) from JST, Japan.

Appendix A: COP of the Peltier device

Here, we show COP of the Peltier device. For simplicity, assuming a weak T dependence of the electrical resistivity and Seebeck coefficient, i.e., $\tau(T) \approx 0$, in Eq. (12), the applied power is given by

$$\begin{aligned}
 P_{\text{electrical}} &= A \int_0^L \frac{d(-J_Q)}{dx} dx \\
 &= -A \int_0^L E_x J dx \\
 &= -A \int_0^L \left(\rho J^2 + S \frac{dT}{dx} J \right) dx \\
 &= -\left(RI^2 + S \Delta T I \right), \tag{A1}
 \end{aligned}$$

where we use $E_x = \rho J + S (dT/dx)$ and $\int_0^L (dT/dx) dx = \int_{T_c}^{T_h} dT = \Delta T$ in Fig. 2 (a). On the other hand, according to Eq. (6), the output heat powers are calculated by

$$\begin{aligned}
 Q_h &= -AJ_Q(L) \\
 &= -AST_h J + A\kappa \frac{dT}{dx} \Big|_{x=L} \quad (\text{for heater}), \tag{A2}
 \end{aligned}$$

$$\begin{aligned}
 Q_c &= -AJ_Q(0) \\
 &= -AST_c J + A\kappa \frac{dT}{dx} \Big|_{x=0} \quad (\text{for cooler}). \tag{A3}
 \end{aligned}$$

According to Eq. (41) for $\langle \tau \rangle_T J x / \langle \kappa \rangle_T \ll 1$, a local temperature in the Peltier device is

$$T(x) = -\frac{\rho J^2}{2\kappa} x^2 + \left(\frac{\Delta T}{L} + \frac{\rho J^2}{2\kappa} L \right) x + T_c, \tag{A4}$$

$$\frac{dT}{dx} = -\frac{\rho J^2}{\kappa} x + \frac{\Delta T}{L} + \frac{\rho J^2}{2\kappa} L, \tag{A5}$$

which gives

$$Q_h = -ST_h I + K \Delta T - \frac{1}{2} RI^2 \quad (\text{for heater}), \tag{A6}$$

$$Q_c = -ST_c I + K \Delta T + \frac{1}{2} RI^2 \quad (\text{for cooler}), \tag{A7}$$

and then the power applied becomes $P_{\text{electrical}} = -(Q_h - Q_c)$. Then, each COP is calculated by

$$\phi_P^{(h)} = \frac{Q_h}{P_{\text{electrical}}} = \frac{ST_h I - K \Delta T + \frac{1}{2} RI^2}{RI^2 + S \Delta T I} \quad (\text{for heater}), \tag{A8}$$

$$\phi_P^{(c)} = \frac{Q_c}{P_{\text{electrical}}} = \frac{ST_c I - K \Delta T - \frac{1}{2} RI^2}{RI^2 + S \Delta T I} \quad (\text{for cooler}). \tag{A9}$$

Appendix B: Boundary conditions: q_{ex} vs. ΔT

Here, we compare two different thermal boundary conditions to calculate a local temperature $T(x)$ in a thermoelectric

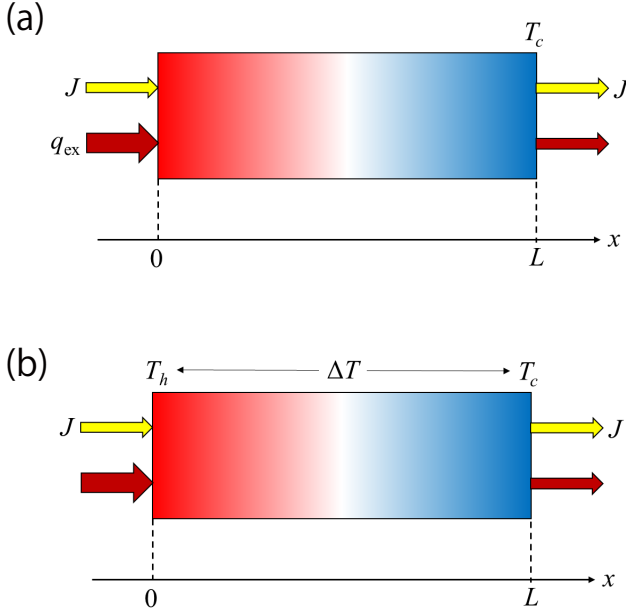


FIG. 8. (a) Boundary condition for a fixed heat current density: $J_Q(x=0) = q_{\text{ex}}$ and $T(x=L) = T_c$. (b) Boundary condition for a fixed temperature difference: $T(x=0) = T_h = \Delta T + T_c$ and $T(x=L) = T_c$. The detail of these definitions are described in the text.

element. For simplicity, assuming a weak T dependence of electrical resistivity and Seebeck coefficient, i.e., $\tau(T) \approx 0$, we solve the following heat equation

$$\frac{d^2 T}{dx^2} = -\frac{\rho J^2}{\kappa}, \quad (\text{B1})$$

which gives

$$T(x) = -\frac{\rho J^2}{2\kappa} x^2 + Ax + B, \quad (\text{B2})$$

where the constant A and B are determined by the boundary conditions for the local temperature $T(x)$ and the heat current density $J_Q(x)$.

1. Boundary condition for a given q_{ex}

First, we assume that a heat current density

$$J_Q(x=0) = q_{\text{ex}} \quad (\text{B3})$$

is injected into the Thomson device at $x=0$ in Fig. 8 (a). We also assume that the Thomson device connects to a heat

bath with $T = T_c$ at $x=L$, which corresponds to the thermal boundary condition

$$T(x=L) = T_c. \quad (\text{B4})$$

The above boundary condition gives

$$\begin{aligned} T(x) = & -\frac{\rho J^2}{2\kappa} x^2 \\ & + \frac{SJ}{\kappa + SJL} \left(T_c + \frac{\rho J^2 L^2}{2\kappa} + \frac{q_{\text{ex}} L}{\kappa} \right) x - \frac{q_{\text{ex}} L}{\kappa} x \\ & + \frac{\kappa}{\kappa + SJL} \left(T_c + \frac{\rho J^2 L^2}{2\kappa} + \frac{q_{\text{ex}} L}{\kappa} \right). \end{aligned} \quad (\text{B5})$$

Then, a generated temperature difference is calculated by

$$\begin{aligned} \Delta T \equiv & T(0) - T_c \\ = & \frac{L}{\kappa + SJL} \left(-ST_c J + \frac{\rho J^2 L}{2} + q_{\text{ex}} \right). \end{aligned} \quad (\text{B6})$$

2. Boundary condition for a given ΔT

Next, we assume that the thermoelectric element is sandwiched by heat baths: one at $x=0$ side has $T = T_h$ and the other at $x=L$ side has $T = T_c$, which corresponds to the thermal boundary condition

$$T(x=0) = T_h, \quad T(x=L) = T_c. \quad (\text{B7})$$

The above boundary condition gives

$$T(x) = -\frac{\rho J^2}{2\kappa} x^2 + \left(-\frac{\Delta T}{L} + \frac{\rho J^2}{2\kappa} L \right) x + T_h. \quad (\text{B8})$$

Then, by using Eq. (6) and $T(0) = T_h = \Delta T + T_c$, let us calculate the heat current density at $x=0$

$$\begin{aligned} J_Q(0) = & ST(0)J - \kappa \frac{dT}{dx} \Big|_{x=0} \\ = & ST_c J - \frac{\rho J^2 L}{2} + \frac{\kappa + SJL}{L} \Delta T. \end{aligned} \quad (\text{B9})$$

Accordingly, the temperature difference is given by

$$\Delta T = \frac{L}{\kappa + SJL} \left(-ST_c J + \frac{\rho J^2 L}{2} + J_Q(0) \right). \quad (\text{B10})$$

Therefore, in the case of $J_Q(0) = q_{\text{ex}}$, Eqs. (B6) and (B10) are equivalent. In other words, when q_{ex} and ΔT are determined, the formulation is independent of the above thermal boundary conditions.

[1] D.M. Rowe, "CRC Handbook of Thermoelectrics," (CRC Press, Boca Raton, 1995).

[2] L. B. Bell, "Cooling, heating, generating power, and recovering waste heat with thermoelectric systems," Science **321**, 1457

- (2008).
- [3] C. Goupil, W. Seifert, K. Zabrocki, E. Müller, and G. J. Snyder, “Thermodynamics of Thermoelectric Phenomena and Applications,” *Entropy* **13**, 1481 (2011).
- [4] W. Liu, Q. Jie, H. S. Kim, and Z. F. Ren and G. Chen, “Current progress and future challenges in thermoelectric power generation: From materials to devices,” *Acta Mater.* **87**, 357 (2015).
- [5] Y. Li, W. Li, T. Han, X. Zheng, J. Li, B. Li, S. Fan, and C.-W. Qiu, “Transforming heat transfer with thermal metamaterials and devices,” *Nat. Rev. Mater.* **6**, 488 (2021).
- [6] H. S. Kim, W. Liu, G. Chen, C. W. Chu, and Z. Ren, “Relationship between thermoelectric figure of merit and energy conversion efficiency,” *Proc. Natl. Acad. Sci. USA* **112**, 8205 (2015).
- [7] R. Modak, M. Murata, D. Hou, A. Miura, R. Iguchi, B. Xu, R. Guo, J. Shiomi, Y. Sakuraba, and K. Uchida, “Phase-transition-induced giant Thomson effect,” *Appl. Phys. Rev.* **9**, 011414 (2022).
- [8] K. Uchida, M. Murata, A. Miura, and R. Iguchi, “Observation of the Magneto-Thomson Effect,” *Phys. Rev. Lett.* **125**, 045202 (2020).
- [9] G. J. Snyder, E. S. Toberer, R. Khanna, and W. Seifert, “Improved thermoelectric cooling based on the Thomson effect,” *Phys. Rev. B* **86**, 045202 (2012).
- [10] W. Seifert, G. J. Snyder, E. S. Toberer, C. Goupil, K. Zabrocki, and E. Müller, “The self-compatibility effect in graded thermoelectric cooler elements,” *Phys. Status Solidi A*, **210**, 1407 (2013).
- [11] V. Bubanja, Y. Amagai, K. Okawa, and N.-H. Kaneko, “Mathematical Modeling and Measurement of Low Frequency Characteristics of Single-Junction Thermal Converters,” *IEEE Trans Instrum Meas* **71**, 1500704 (2022).
- [12] Y. Amagai, T. Shimazaki, K. Okawa, H. Fujiki, T. Kawae, and N.-H. Kaneko, “Precise measurement of absolute Seebeck coefficient from Thomson effect using ac-dc technique,” *AIP Adv.* **9**, 065312 (2019).
- [13] I. T. Witting, T. C. Chasapis, F. Ricci, M. Peters, N. A. Heinz, G. Hautier, and G. J. Snyder, “The thermoelectric properties of bismuth telluride,” *Adv. Electron. Mater.* **5**, 1800904 (2019).
- [14] N. F. Hinsche, F. Rittweger, M. Hölzer, P. Zahn, A. Ernst, and I. Mertig, “Ab initio description of the thermoelectric properties of heterostructures in the diffusive limit of transport,” *Phys. Status Solidi A*, **213**, 672 (2016).
- [15] A. K. Bohra, R. Bhatt, A. Singh, S. Bhattacharya, R. Basu, K. N. Meshram, S. K. Sarkar, P. Bhatt, P. K. Patro, D. K. Aswal, *et al.*, “Transition from n- to p-type conduction concomitant with enhancement of figure-of-merit in Pb doped bismuth telluride: Material to device development,” *Mater. Des.* **159**, 127 (2018).
- [16] J. Kudrnovský, V. Drchal, and I. Turek, “Physical properties of FeRh alloys: The antiferromagnetic to ferromagnetic transition,” *Phys. Rev. B* **91**, 014435 (2015).
- [17] P. A. Algarabel, M. R. Ibarra, C. Marquina, and A. del Moral, “Giant room-temperature magnetoresistance in the FeRh alloy,” *Appl. Phys. Lett.* **66**, 3061 (1995).
- [18] S. Mankovsky, S. Polesya, K. Chadova, H. Ebert, J. B. Staunton, T. Gruenbaum, M. A. W. Schoen, C. H. Back, X. Z. Chen, and C. Song, “Temperature-dependent transport properties of FeRh,” *Phys. Rev. B* **95**, 155139 (2017).
- [19] D. Hsieh, D. Qian, L. Wray, Y. Xia, Y. S. Hor, R. J. Cava, and M. Z. Hasan, “A topological Dirac insulator in a quantum spin Hall phase,” *Nature* **452**, 970 (2008).
- [20] W. M. Yim and A. Amith, “Bi-Sb alloys for magneto-thermoelectric and thermomagnetic cooling,” *Solid State Electron.* **15**, 1141 (1972).
- [21] M. Murata, A. Yamamoto, Y. Hasegawa, and T. Komine, “Magnetic-Field Dependence of Thermoelectric Properties of Sintered Bi₉₀Sb₁₀ Alloy,” *J. Electron. Mater.* **45**, 1875 (2016).
- [22] Y. Satake, J. Shiogai, G. P. Mazur, S. Kimura, S. Awaji, K. Fujiwara, T. Nojima, K. Nomura, S. Souma, T. Sato, T. Dietl, and A. Tsukazaki, “Magnetic-field-induced topological phase transition in Fe-doped (Bi,Sb)₂Se₃ heterostructures,” *Phys. Rev. Materials* **4**, 044202 (2020).
- [23] T. Chiba and S. Takahashi, “Transport properties on an ionically disordered surface of topological insulators: Toward high-performance thermoelectrics,” *J. Appl. Phys.* **126**, 245704 (2019).